Chin. J. Astron. Astrophys. Vol. 4 (2004), No. 1, 51–60
(http://www.chjaa.org or http://chjaa.bao.ac.cn)

Chinese Journal of
Astronomy and
Astrophysics

Determination of the Thickness of Non-Edge-on Disk Galaxies

Ying-He Zhao[1], Qiu-He Peng[1,2,3] and Lan Wang[1]

[1] Department of Astronomy, Nanjing University, Nanjing 210093; qhpeng@nju.edu.cn
[2] Joint Astrophysics Center of Chinese Academy of Science-Peking University, Beijing 100871
[3] The Open Laboratory of Cosmic Ray and High Energy Astrophysics, Chinese Academy of Sciences

Received 2003 June 9; accepted 2003 September 3

Abstract We propose a method to determine the thickness of non-edge-on disk galaxies from their observed structure of spiral arms, based on the solution of the truly three-dimensional Poisson's equation for a logarithmic disturbance of density and under the condition where the self-consistency of the density wave theory is no longer valid. From their measured number of arms, pitch angle and location of the innermost point of the spiral arms, we derive and present the thicknesses of 34 spiral galaxies.

Key words: galaxies: non-edge-on galaxies — galaxies: spiral — thickness: density wave theory

1 INTRODUCTION

On the basis of isothermal disk models, Van der Kruit & Searle (1981a, b; 1982a, b) developed a method for determining the scale heights of disk galaxies observed edge-on. This method is based on fitting the distribution of the surface brightness of disk galaxies by a radial exponential distribution. Peng et al. (1979) examined the solution of the three-dimensional Poisson's equation of spiral galaxies using Green function and Bessel-Fourier transformation. They obtained an integral expression and an asymptotic formula for the self-gravitational potential of the logarithmic spiral arms due to some given logarithmic disturbance of the matter density. On the basis of this theory, Peng (1988) proposed a method of determining the thickness of non-edge-on spiral galaxies (from the observed number of spiral arms, the pitch angle and the location of the innermost point of the arms). However, the rough method used in that paper is questionable because it incorrectly extended the asymptotic formula for the disturbed gravitational potential right through to the galactic center (Peng et al. 2003). In fact, the arms only exist in the area $r > r_0$ (r_0 is the forbidden radius of density wave). In this paper we correct this mistake and re-estimate the scale height of spiral galaxies on the basis of the exact integral representation for the disturbed gravitational potential (see equation (A) of Peng et al. (1979) or Eq. (A19) in the appendix of this paper).

2 THE DISTURBED GRAVITATIONAL POTENTIAL

The density distribution along the z-direction for a finitely thick galaxy is

$$\rho(r,\theta,z)=\rho(r,\theta,0)e^{-\alpha|z|}=\frac{\alpha}{2}\sigma(r,\theta)e^{-\alpha|z|}, \tag{1}$$

where $\alpha=2/H$, H being the effective thickness of the galaxy, and $\sigma(r,\theta)$ is the surface density, which includes the basic surface density of the disk and the disturbance density: $\sigma(r,\theta)=\sigma_0(r)+\sigma_1(r,\theta,t)$. Taking a logarithmic disturbance of density (Danver 1942; Kennicutt & Hodge 1982; Peng 1988),

$$\sigma_1(r,\theta,t)=\frac{A}{r}e^{i\Lambda\ln(r)}e^{i(\omega t-m\theta)}, \tag{2}$$

where m is the number of arms in the galaxy, A is a parameter measuring the intensity of the density disturbance and $\Lambda=m\cot\mu$ quantifies the winding level of the logarithmic spiral, μ being the pitch angle of the arms. The gravitational potential generated by the density disturbance can be found by solving the three-dimensional Poisson's equation

$$\nabla^2V_1(r,\theta,z,t)=-2\pi G\alpha\sigma_1(r,\theta,t)e^{-\alpha|z|}. \tag{3}$$

A rigorous solution of the potential on the galactic plane ($z=0$) was found (Peng et al. 1979),

$$V_1(r,\theta,0,t)=-2\pi GAe^{i[\omega t-m\theta+\Lambda\ln(r)]}\mathrm{Re}\{g(\alpha r)\}, \tag{4}$$

where

$$g(\alpha r)=e^{i\Lambda\ln 2}\frac{\Gamma(\frac{1+m+i\Lambda}{2})}{\Gamma(\frac{1+m-i\Lambda}{2})}\int_0^\infty J_m(x)\frac{e^{-i\Lambda\ln x}}{x(1+\frac{x}{\alpha r})}dx, \tag{5}$$

with $\Gamma(x)$ and $J_m(x)$ being the usual Gamma function and Bessel function, respectively. For an infinitely thin disk, the potential may be reduced to the expression given by Kalnajs (1971)

$$V_1(r,\theta,t)=-2\pi GAe^{i[\omega t-m\theta+\Lambda\ln(r)]}\frac{1}{\sqrt{m^2+\Lambda^2}}. \tag{6}$$

3 THE SELF-CONSISTENT DENSITY WAVE & THE FORBIDDEN RADIUS OF DENSITY WAVE

According to the self-consistent theory of density wave (Lin & Shu 1964), the pattern of spiral arms persists self-consistently only when the intensity of the "induced" gravitational potential solved by Poisson's Equation is equal to the "introduced" gravitational potential, which is the disturbed potential in the Jeans equation for the stellar system of the galaxy. This theory is suitable for an infinitely thin disk. However, for the same density disturbance, the amplitude of the induced gravitational disturbance for disks with a finite thickness is weaker than for the infinitely thin disk and that the thicker the disk, the greater is the difference (Luo & Peng 1999). In this condition, the self-consistency of density wave no longer holds in the central region. The "induced" potential is too weak to excite disturbance of matter corresponding to the original disturbance intensity, and this leads to the disappearance of the spiral pattern in the central region. Therefore, arms that exist in the outer part of the galactic disk can only extend inward to a certain point and not all the way to the center. In other words, there will be no patterns of spiral arms in the central part of a finitely thick disk (Peng et al. 2003). The area with no spiral pattern of density waves is the so-called "forbidden region of density wave". Let r_0 denote the forbidden region radius.

Observationally, the forbidden region radius r_0 can be measured directly by estimating the innermost point that the arms reach to. Theoretically, when the amplitude of the "induced" gravitational potential has decreased to a certain degree below the value for the infinitely thin disk, the disturbance density corresponding to the original disturbance can no longer be excited. This can be used to determine the forbidden region radius. A feasible method is to establish an "objective" criterion for the ceasing of validity of self-consistency of density wave (i.e., the disappearance of the pattern of spiral arms) by checking galaxies with given scale heights. Now, the Milky Way and M31 (Andromeda galaxy, NGC 224) are the two galaxies that have been thoroughly studied and their scale heights have been well determined. We therefore use their well determined relevant parameters to identify the criterion we want. Specifically, the parameters are the number of arms m, the winding parameters Λ and the innermost point of the arms r_0. They are listed in Table 1.

Table 1 Parameters of the Milky Way & M31

Name	m	Λ	r_0 (kpc)	H (kpc)	α
Milky Way	2	14.0	4.5	0.65	3.07
Milky Way	4	14.0	4.5	0.65	3.07
Milky Way	4	14.0	4.0	0.65	3.07
Milky Way	4	18.8	4.5	0.65	3.07
M31	2	14.8	7.5	0.80	2.5

At the point r_0, the amplitude ratio of the disturbed gravitational potential of finitely thick disk to infinitely thin disk is

$$\eta = \frac{V_\alpha(\alpha, m, \Lambda, r_0)}{V_{\alpha\to\infty}(m, \Lambda)} = \frac{-2\pi G A e^{i[\omega t - m\theta + \Lambda \ln(r)]}\mathrm{Re}\{g(\alpha r)\}}{-2\pi G A e^{i[\omega t - m\theta + \Lambda \ln(r)]}\frac{1}{\sqrt{m^2+\Lambda^2}}} = \mathrm{Re}\{g(\alpha r_0)\}\sqrt{m^2 + \Lambda^2}. \qquad (7)$$

We presume that the disturbed gravitational potential could excite exactly the density wave when at a certain value. Calculating this value for the Milky Way and M31 with their known thickness (Peng et al. 2003), we have Milky Way: $\eta = \begin{cases} 0.496 & \mathrm{m}=2 \\ 0.487 & \mathrm{m}=4 \end{cases}$; M31: $\eta = 0.556$.

We have chosen the mean value $\bar{\eta} = 0.50$ as the condition at which the self-consistency of the density wave theory ceases to be valid. That is, in the area where the amplitude of the induced gravitational potential has decreased to less than 50% of the introduced gravitational potential, the corresponding density wave cannot be excited, and this leads to the disappearance of the density wave and the pattern of spiral arms. Thus we define the point at which the ratio of Eq. (7) decreases to 50% as the radius of "the forbidden region of density wave" (Peng et al. 2003). We must point out here that the most probable range of the reduction factor η is $0.45 \sim 0.55$ according to our calculations on the two galaxies and the average value, 0.5, which we took would mean a 10% error when estimating the galaxy thickness. This 10% error would be superposed on other possible sources of error. The criterion for determining the radius of the forbidden region for the propagation of density waves has been previously considered by Peng et al. (1979) and Peng (1988). In particular, we note that for $\alpha r \gg \sqrt{\Lambda^2 + m^2}$ or in the region defined by $r \gg \sqrt{\Lambda^2+m^2}/\alpha = H\sqrt{\Lambda^2+m^2}/2$, it is possible to derive an asymptotic representation for the approximate disturbed gravitational potential $V_1(r, \theta, z=0, t)$ from the asymptotic expansion for the function $g(\Lambda, m; \alpha r)$ as given by Eq. (5) of this paper:

$$V_1(r,\theta,z=0,t) \approx -2\pi GA\Big(\frac{1}{\sqrt{\Lambda^2+m^2}} - \frac{1}{\alpha r}\Big)e^{i(\omega t+\Lambda \ln r - m\theta)}. \tag{8}$$

The zero point for this asymptotic expression is given by

$$r = r_0' = \frac{\sqrt{\Lambda^2+m^2}}{\alpha} = \frac{H}{2}\sqrt{\Lambda^2+m^2}. \tag{9}$$

In Peng et al. (1979) and Peng (1988), the authors inappropriately extended the disturbed gravitational potential given by Eq. (8) to the region $r < r_0'$. They incorrectly considered that the sign of the disturbed gravitational potential (see Eq. (4)) in the region defined by $r < r_0'$ would be opposite to that in the region defined by $r > r_0'$. In other words, the phase of the disturbed gravitational potential was the same as the phase of the density disturbance. Starting from the principle that the phase of the disturbed gravitational potential is opposite to that of the density disturbance (Lin & Shu 1964), Peng et al. (1979) and Peng (1988) concluded that the spiral arms of density waves cannot appear in the central region defined by $r < r_0'$. That is, r_0' is the innermost point that the spiral arms can reach and that at this point the value of η is zero.

In particular, we note that the approximate asymptotic expression Eq. (8) is valid provided that $(\alpha r)^2 \gg \Lambda^2 + m^2$. The rigorous integral expression of the function $g(\Lambda, m; \alpha r)$ was computed numerically and we found that the real part of the function $g(\Lambda, m, \alpha r_0')$ at the point r_0' is obviously greater than zero (Luo et al. 1999). However, at the point r_0', the ratio η as defined by Eq. (7) has approximately the value $\eta \cong 0.5$. Thus, the method for determining the thickness (or scale height) of non-edge-on spiral galaxies proposed by Peng (1988) has apparent shortcomings. Accodingly, we have in this paper carefully revised and reinvestigated the key factors concerning the central forbidden zone for the propagation of spiral density waves in disk galaxies with finite thickness.

4 MEASUREMENTS AND RESULTS

The sample of galaxies used in this paper is part of the 60 spiral galaxies in table 1 of Ma (2001). Because of lack of the radial velocity or some other parameters, the thicknesses of 26 of the galaxies cannot be calculated. So, the sample of this paper includes only 34 non-edge-on spiral galaxies.

We calculate the thickness parameter, α, through Eq. (7) by taking $\eta = 0.5$ at first, then h and H can be calculated. The errors of our calculation mainly come from: a) the position of the starting point of the arm; b) the inclination of the galaxy; c) the position of the galactic center; d) the parameter η. The errors from the positions of the arm starting point and of the center, however, can be decreased if the grey-scale of an image is modified properly using IRAF to obtain the deep possible fine structure of the galaxy. The error estimates are derived from the formulae by Peng (1988) and Shang et al. (1992). The scale heights (H) of these spiral galaxies and their relative errors are listed in Table 2. Table 2 also includes the following parameters: the number of arms m, the mean numerical Hubble type T (=1, 2, 3, 4, 5 for Sa, Sab, Sb, Sbc, Sc and Scd, respectively), the radius of the forbidden region r_0 (with errors $\pm 0.05'$) or the radius of the starting point of the arms, the winding parameter of the arms $\Lambda (= m \cot\mu)$, obtained by fitting the observed image of the arms by logarithmic curves (Peng 1988; Ma 2001), the radial velocity of the galaxy v from $RC3$, its distance D, calculated according to Hubble's Law (with a Hubble constant, H_0, of 71 km s^{-1} Mpc^{-1}) the apparent scale height of the galaxy

h, and its flatness H/D_0, (D_0 is the isophotal major diameter corrected to "face-on", and for Galactic extinction to A_g=0, but not for redshift).

Table 2 Thicknesses of 34 Spiral Galaxies

No.	m	T	r_0 ($'$)	$\Lambda \pm d\Lambda/\Lambda$	v (km s^{-1})	D (Mpc)	$h \pm dh/h$ ($'$)	$H \pm dH/H$ (kpc)	H/D_0
PGC00303	2	3.0	0.118	2.86±16.5%	4639	65.34	0.0655±63.4%	1.244±63.4%	0.041
PGC 02949	2	1.5	0.48	9.89±19.1%	3770	53.10	0.0945±38.5%	1.459±38.5%	0.041
PGC 05939	2	3.3	0.444	18.68±75.3%	4861	68.46	0.0472±95.4%	0.939±95.4%	0.026
PGC 06833	2	5.0	0.215	4.26±8.1%	2661	37.48	0.0891±39.7%	0.971±39.7%	0.030
PGC 08961	2	3.0	0.203	2.89±19.9%	7335	103.31	0.1119±48.0%	3.361±48.0%	0.049
PGC 09236	2	5.3	0.289	6.57±20.6%	1266	17.83	0.0830±45.7%	0.430±45.7%	0.021
PGC 10488	2	3.0	2.476	10.65±7.4%	1103	15.54	0.4542±19.1%	2.053±19.1%	0.048
PGC 13584	2	3.0	0.408	8.75±18.7%	3959	55.76	0.0901±39.7%	1.462±39.7%	0.033
PGC 14897	2	4.0	0.588	5.77±4.8%	1472	20.73	0.1893±22.7%	1.142±22.7%	0.023
PGC 15018	2	3.0	0.659	3.05±9.5%	2404	33.86	0.3500±67.8%	3.447±24.1%	0.067
PGC 18709	2	3.0	0.439	14.01±33.4%	4053	57.08	0.0618±53.9%	1.026±53.9%	0.027
PGC 23028	2	3.0	0.395	10.07±46.3%	2649	37.31	0.0764±66.6%	0.829±66.6%	0.031
PGC 24723	2	3.0	0.549	10.51±53.9%	2203	31.03	0.1020±70.5%	0.921±70.5%	0.042
PGC 30323	2	3.5	0.487	4.6±9.6%	3148	44.34	0.1897±28.1%	2.447±42.2%	0.079
PGC 31926	2	3.0	0.649	4.28±17.8%	3315	46.69	0.2679±21.8%	3.639±21.8%	0.070
PGC 33410	2	5.0	0.56	13.97±50.2%	1537	21.65	0.0791±47.8%	0.498±47.8%	0.026
PGC 33860	2	4.0	0.187	5.44±16.2%	2423	34.13	0.0633±50.6%	0.629±50.6%	0.022
PGC 34232	2	3.0	0.471	5.3±20.3%	2345	33.03	0.1631±37.8%	1.567±37.8%	0.058
PGC 36875	2	5.0	0.463	8.05±7.4%	1178	16.59	0.1105±27.6%	0.533±27.6%	0.025
PGC 38240	2	3.5	0.242	9.76±12.2%	6439	90.69	0.0482±42.2%	1.272±42.2%	0.022
PGC 39479	2	5.0	0.22	8.91±58.9%	4065	57.25	0.0478±87.9%	0.796±87.9%	0.020
PGC 47404	2	4.0	0.599	6.68±3.1%	640	9.01	0.1695±21.1%	0.444±21.1%	0.015
PGC 48130	2	4.0	0.45	4.53±11.3%	1437	20.24	0.1775±30.3%	1.045±30.3%	0.029
PGC 48371	2	4.5	0.239	11.39±18.2%	6806	95.86	0.0411±48.4%	1.146±48.4%	0.025
PGC 49881	2	3.0	0.406	5.9±13.1%	3134	44.14	0.1282±33.7%	1.646±33.7%	0.059
PGC 51169	2	5.0	0.219	14.87±20.5%	6924	97.52	0.0291±52.8%	0.825±50.8%	0.011
PGC 54018	2	4.5	0.17	7.03±24.6%	3209	45.20	0.0459±61.7%	0.604±61.7%	0.020
PGC 54097	2	5.0	0.244	8.3±12.4%	2081	29.31	0.0566±42.0%	0.483±42.0%	0.017
PGC 54445	2	3.0	0.403	3.61±11.9%	3461	48.75	0.1897±31.3%	2.690±31.3%	0.048
PGC 64652	2	4.0	0.115	5.82±20.6%	4581	64.52	0.0367±71.4%	0.690±71.4%	0.016
PGC 65086	2	4.0	0.445	3.98±4.2%	1280	18.03	0.1945±24.5%	1.020±24.5%	0.041
PGC 65269	2	3.0	0.262	4.16±20%	4368	61.52	0.1106±44.8%	1.980±44.8%	0.051
PGC 69439	2	4.0	0.244	5.17±11.5%	4404	62.03	0.0863±40.2%	1.557±40.2%	0.042
PGC 72387	2	4.0	0.44	8.18±12.2%	4837	68.13	0.1035±32.7%	2.051±32.7%	0.030

5 DISCUSSION

5.1 The Value of η

Until now, only the scale heights of two spiral galaxies, the Milky Way and M31, are well established and we have no other means to determine the value of η more precisely. We will do more work on this point and try to find another individual way to determine the thickness of spiral galaxies and to check whether our adopted value of η is suitable. We note that the difference between the thicknesses obtained by the method of this paper and by the method proposed in Peng (1988) is very small, it is less than 5%. Since the total error in the evaluation of the thickness from all possible sources of error is apparently larger than 10%, the earlier method of Peng (1988), although inaccurate from a theoretical point of view, is still basically valid. In other words, the approximate asymptotic expression given by Eq. (9) for the radius of the central forbidden region is essentially valid. Alternatively, we may compute the thickness of spiral galaxy in terms of the number of spiral arms m, the winding parameter Λ and the radius r_0 for the forbidden region through the simple formula

$$H = \frac{2r_0}{\sqrt{\Lambda^2 + m^2}}, \tag{10}$$

then we can use the value of H so obtained to calculate the value of the reduction factor from Eq. (7) at the forbidden radius r_0 and test whether the criterion $\eta < 0.5$ is satisfied.

5.2 Some Properties of Spiral Galaxies

Ma (2002) has studied some statistical correlations between the properties of disks and of spiral arms with some physical properties of galaxies. The main conclusions are that the thickness of spiral disks is correlated with the Hubble sequence and that there exists correlations between arm pattern and total luminosity, total surface densities and I linewidths (see details in Ma 2002). In this section we will show some new correlations between the properties of galaxy disks and of spiral arms with some physical properties of galaxies.

a) Figure 1 plots the thicknesses of the galaxies versus their distance. There is no obvious correlation between these two parameters. The disks of spiral galaxies are mainly thin disks. From Table 2 we can see that spiral galaxies of the same Hubble type have about the same value of flatness (H/D_0). The mean value of flatness is 0.046, 0.026 and 0.021 for Sb ($T = 2.0$), Sbc ($T = 3.0$) and Sc ($T = 4.0$) spirals, respectively: there is a trend of spirals getting flatter along the Hubble sequence Sb–Sc.

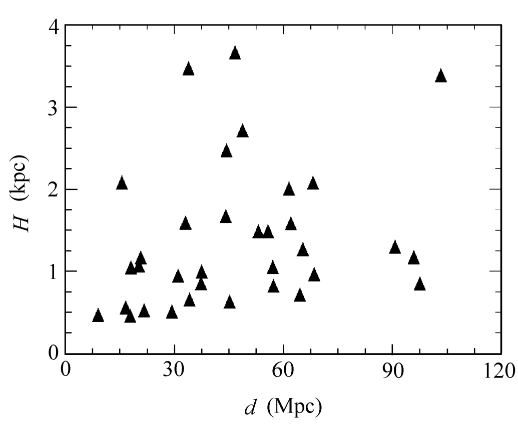

Fig. 1 Thickness versus distance plot of spiral galaxies.

b) Figure 2 presents the correlations between r_0 (kpc) and H. It shows that the thicker the galaxy disk is, the larger the forbidden region radius becomes. In other words, the role played by the thickness of the galaxy is to push the region where the spiral density waves first appear outward (relative to the galactic center). This reflects the fact that the disturbed gravitational potential due to the disturbed matter density is not synchronized at higher z and at the galactic plane $z = 0$. The thicker the galaxy disk, the weaker is the disturbed gravitational potential in the central area, and this leads to a bigger region with no density wave pattern.

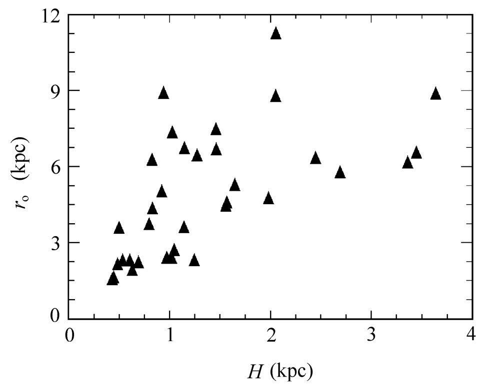

Fig. 2 Forbidden radius of spiral galaxy plotted versus the thickness.

c) As shown in Figure 3, spiral galaxies with larger winding parameters Λ have larger radii r_0 of the central forbidden region. A qualitative description of this scenario is that the spiral arms of a tightly winding spiral structure will appear far out from the galactic center, whereas a loosely winding spiral structure may extend to the galactic center. This striking tendency is clearly revealed in the classic Hubble classification of galaxies.

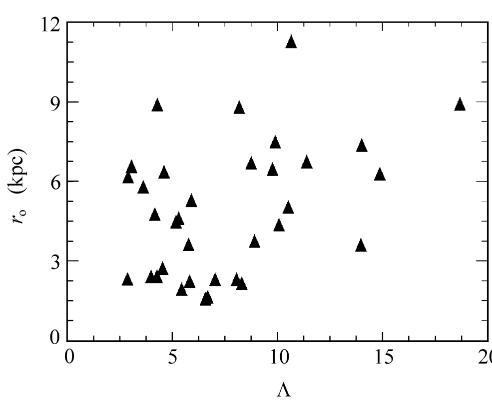

Fig. 3 Forbidden radius of spiral galaxy plotted versus the winding parameter.

d) Figure 4 shows the correlations between the winding parameter Λ and the thickness H. The thicker the galaxy, the smaller winding parameter is. This correlation could be easily deduced from our above discussions b) and c).

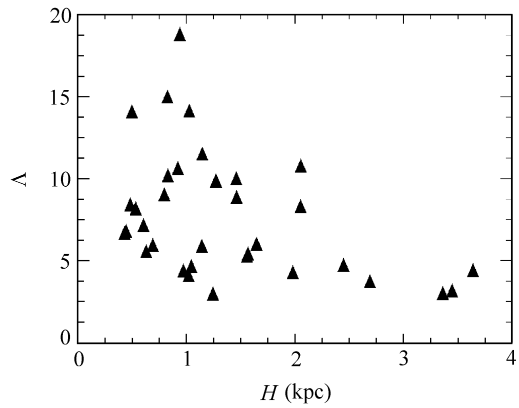

Fig. 4 Winding parameter of spiral galaxy plotted versus the thickness.

APPENDIX

When studying the effect of finite thickness of the disk on the dynamical properties of disk galaxies, it is convenient to adopt the cylindrical coordinates (r, θ, z) with origin at the galactic center, z the distance above the galactic plane, and θ the azimuthal coordinate. For disk galaxies with zero-thickness, the self-gravitational potential Φ is governed by Poisson's equation

$$\nabla^2\Phi = 4\pi G\sigma(r,\theta)\delta(z), \tag{A1}$$

where G is the gravitational constant, ∇^2 the Laplacian operator, $\delta(z)$ Dirac's delta function and $\sigma(r, \theta)$ the surface density. For regions outside the galactic plane $z \neq 0$, Eq. (A1) becomes

$$\nabla^2\Phi(r,\theta,z) = 0, \tag{A2}$$

since there is no distribution of matter outside the disk plane. It is particularly convenient at this point to introduce the Laplace transform for the vertical coordinate z and the Fourier transform for the azimuthal angle θ, namely

$$\Phi(r,\theta,z) = e^{-im\theta}\int_0^\infty U_\beta(r)e^{-\beta|z|}d\beta. \tag{A3}$$

Applying these transformations to Eq. (A2) we then have

$$x\frac{d}{dx}(x\frac{dU_\beta(x)}{dx}) + (x^2 - m^2)U_\beta(x) = 0\,, \tag{A4}$$

where $x = \beta r$, and the solution to Eq. (A4) is the well known Bessel function of order m

$$U_\beta(x) \equiv U(\beta r) = -J_m(\beta r)\,. \tag{A5}$$

Using Eq. (A5) in Eq. (A3), we obtain

$$\Phi(r,\theta,z) = e^{-im\theta}\int_0^\infty [-J_m(\beta r)]\,e^{-\beta|z|}d\beta\,. \tag{A6}$$

On the other hand, we may integrate Poisson's equation (Eq. (A1)) with respect to z to obtain the following expression for the surface density $\sigma(r,\theta)$

$$\sigma(r,\theta) = \frac{1}{4\pi G}\Big\{\Big[\frac{\partial\Phi}{\partial z}\Big]_{0^+} - \Big[\frac{\partial\Phi}{\partial z}\Big]_{0^-}\Big\}\,. \tag{A7}$$

Substituting Eq. (A6) in Eq. (A1) and Eq. (A7) we can recast Poisson's equation for disk galaxies with zero thickness in the form

$$\nabla^2\left\{\int_0^\infty e^{-im\theta}\left[-J_m(\beta r)\right]e^{-\beta|z|}d\beta\right\} = \int_0^\infty e^{-im\theta}2\beta J_m(\beta r)\delta(z)d\beta\,, \tag{A8}$$

$$\nabla^2[J_m(\beta r)e^{-im\theta-\beta|z-z'|}] = -2\beta J_m(\beta r)e^{-im\theta}\delta(z-z')\,. \tag{A9}$$

On the basis of the above mathematical treatment and the standard method of Green function, it is straightforward to derive the appropriate Poisson equation for the three-dimensional disk galaxies with finite thickness

$$\nabla^2\Psi(r,\theta,z) = 4\pi G\rho(r,\theta,z)\,, \tag{A10}$$

where the vertical distribution of matter is described by Parenago's law, $\rho(r,\theta,z) = \frac{\alpha}{2}\sigma(r,\theta)e^{-\alpha|z|}$ (see Eq. (1) in the text). The disturbed surface density for spiral galaxies with spiral arms m may be written as $\sigma^{(m)}(r,\theta) = \sigma_m(r)e^{-im\theta}$ (For axisymmetric disks without spiral arms, $m=0$, so that $\sigma^{(0)}(r,\theta) = \sigma_0(r)$). To proceed, we apply the Bessel-Fourier transform to $\sigma_m(r)$ to obtain

$$\sigma_m(r) = \int_0^\infty \beta J_m(\beta r)S_m(\beta)d\beta\,, \tag{A11}$$

$$S_m(\beta) = \int_0^\infty rJ_m(\beta r)\sigma_m(r)dr\,, \tag{A12}$$

where $S_m(\beta)$ is the Bessel-Fourier transform of $\sigma_m(r)$. Substituting Eqs. (A1) and (A11) into Eq. (A10), the three-dimensional Poisson equation can be rewritten as

$$\nabla^2\Psi_m(r,\theta,z) = 2\pi G\alpha e^{-im\theta}\int_{-\infty}^\infty e^{-\alpha|z'|}dz'\int_0^\infty \beta J_m(r\beta)S_m(\beta)\delta(z-z')d\beta\,. \tag{A13}$$

Compare Eq. (A13) with Eq. (A9) we then find the formal solution of the gravitational potential for a galactic disk with scale height $H = 2/\alpha$,

$$\Psi_m(r,\theta,z) = -2\pi Ge^{-im\theta}\int_0^\infty J_m(r\beta)S_m(\beta)F(\alpha,\beta,z)d\beta\,, \tag{A14}$$

where

$$F(\alpha,\beta,z) = \frac{1}{(\frac{\beta}{\alpha})^2-1}\left[\frac{\beta}{\alpha}e^{-\alpha|z|} - e^{-\beta|z|}\right]\,. \tag{A15}$$

Since the spiral arms are mainly confined to the galactic plane $z=0$, we therefore focus our attention to only the gravitational potential on the galactic plane

$$\Psi_m(r,\theta,z=0) = -\pi G\alpha e^{-im\theta}\int \frac{2}{\alpha+\beta}S_m(\beta)J_m(\beta r)d\beta\,. \tag{A16}$$

For a logarithmic spiral density disturbance (see Eq. (2) of the text), we have

$$\sigma_m(r) = \frac{A}{r} e^{i\Lambda \ln r}\,, \tag{A17}$$

$$S_m(\beta) = A 2^{i\Lambda} \frac{\Gamma((1+m+i\Lambda)/2)}{\Gamma((1+m-i\Lambda)/2)} \beta^{-(i\Lambda+1)}\,. \tag{A18}$$

Using Eq. (A18) in Eq. (A16) we then obtain the corresponding disturbed gravitational potential,

$$\Psi_m(r,\theta,z=0,t) = -2\pi G A e^{i(\omega t - m\theta + \Lambda \ln r)} \Re e\{g(\alpha r, \Lambda)\}\,, \tag{A19}$$

where $\Re e\{...\}$ denotes the mathematical operation of taking the real part of the quantity in the bracket $\{...\}$,

$$g(\alpha r, \Lambda) = e^{i\Lambda \ln 2} \frac{\Gamma[(1+m+i\Lambda)/2]}{\Gamma[(1+m-i\Lambda)/2]} \int_0^\infty J_m(x) \frac{e^{-i\Lambda \ln r}}{x[1+x/(\alpha r)]} dx\,, \tag{A20}$$

$\Gamma(x)$ and $J_m(x)$ being the usual Gamma and Bessel functions, respectively. For regions where $\alpha r \gg \sqrt{\Lambda^2+m^2}$ or $r \gg \sqrt{\Lambda^2+m^2}/\alpha = H\sqrt{\Lambda^2+m^2}/2$, we may derive the asymptotic gravitational potential disturbance from Eqs. (A19) and (A20):

$$\Psi_m(r,\theta,z=0,t) \approx -2\pi G A \left(\frac{1}{\sqrt{\Lambda^2+m^2}} - \frac{1}{\alpha r}\right) e^{i(\omega t + \Lambda \ln r - m\theta)}\,. \tag{A21}$$

For a razor thin disk ($\alpha \to \infty$), the potential may be reduced to the very simple expression given by Kalnajs(1971)

$$\Psi_m(r,\theta,0,t) = -\frac{2\pi G A}{\sqrt{m^2+\Lambda^2}} e^{i(\omega t + \Lambda \ln r - m\theta)}\,. \tag{A22}$$

References

Danver C. C., 1942, Ann. Lund. Obs., 10, 162
Kalnajs A. J., 1971, ApJ, 166, 275
Kennicutt R. C., Hodge P., 1982, ApJ, 253, 101
Lin C. C., Shu F. H., 1964, ApJ. 140, 646
Luo X. L., Peng Q. H., Chin. Phys. Lett., 1999, 16, 931
Ma J., 2002, A&A, 388, 389
Ma J., Peng Q. H., Li W. D. et al., 1998, Acta Astrophys. Sin., 18, 11
Ma J., Peng Q. H., Li W. D. et al., 1998, Acta Astron. Sin., 39, 28
Ma J., 2001, Chin. J. Astron. Astrophys., 1, 395
Peng Q. H., 1988, A&A, 206, 18
Peng Q. H., Li X. Q., Su H. J., Huang J. H., 1979, Sci. Sinica, XXII, 925
Peng Q. H., Chou C. K., Zhao Y. H. et al., 2003, MNRAS, submitted
Shang Z. H., Bao M. X., Zhang W. Y. et al., 1992, Acta Astron. Sin., 33, 371
van der Kruit P. C., Searle L., 1981a, A&A, 95, 105
van der Kruit P. C., Searle L., 1981b, A&A, 95, 116
van der Kruit P. C., Searle L., 1982a, A&A, 110, 61
van der Kruit P. C., Searle L., 1982b, A&A, 110, 79